Performance of a finned-tube evaporator optimized for different refrigerants and its effect on system efficiency[☆]

Piotr A. Domanski[*], David Yashar, Minsung Kim

Building and Fire Research Laboratory, National Institute of Standards and Technology, 100 Bureau Drive, Stop 8631, Gaithersburg, MD 20899-8631, USA

Abstract

This paper presents a comparable evaluation of R600a (isobutane), R290 (propane), R134a, R22, R410A, and R32 in an optimized finned-tube evaporator, and analyzes the impact of evaporator effects on the system coefficient of performance (COP). The study relied on a detailed evaporator model derived from NIST's EVAP-COND simulation package and used the ISHED1 scheme employing a non-Darwinian learnable evolution model for circuitry optimization. In the process, 4500 circuitry designs were generated and evaluated for each refrigerant. The obtained evaporator optimization results were incorporated in a conventional analysis of the vapor compression cycle. For a theoretical cycle analysis without accounting for evaporator effects, the COP spread for the studied refrigerants was as high as 11.7%. For cycle simulations including evaporator effects, the COP of R290 was better than that of R22 by up to 3.5%, while the remaining refrigerants performed approximately within a 2% COP band of the R22 baseline for the two condensing temperatures considered.
© 2005 Elsevier Ltd and IIR. All rights reserved.

Keywords: Air conditioning; Refrigerating system; Evaporator; Finned tube; Modelling; Optimization; R600a; R410A; Propane; R32; R134a; R22; Comparison

Performance d'un évaporateur à tubes à ailettes optimisé pour plusieurs frigorigènes et impact sur l'efficacité du système

Mots clés : Conditionnement d'air ; Système frigorifique ; Évaporateur ; Tube aileté ; Modélisation ; Optimisation ; R600a ; R410a ; Propane ; R32 ; R134a ; R22 ; Comparaison

1. Introduction

Increasing concerns about climate change provide a new design factor for conventional systems striving for high efficiency and energy conservation at a given production cost. This new factor is the preference to utilize refrigerants that have a low global warming potential (GWP), with other things being equal. Considering that the system's indirect

Nomenclature

COP	coefficient of performance
G	refrigerant mass flux (kg s^{-1} m^{-2})
GWP	global warming potential
h	enthalpy (kJ kg^{-1})
h_{fg}	latent heat (kJ kg^{-1})
k	thermal conductivity (W m^{-1} K^{-1})
m_r	refrigerant mass flow rate (kg h^{-1})
P	pressure (kPa)
Q	total capacity (kW)
Q_l	latent capacity, portion of total capacity due to water vapor removal (kW)
$s*$	normalized entropy

T_{sat}	saturated temperature at the evaporator exit (°C)
x	vapor quality
μ	viscosity (µPa s)
ρ	density (kg m^{-3})

Subscript

f	saturated liquid
g	saturated vapor
in	evaporator inlet
out	evaporator outlet

contribution to climate change (CO_2 emissions from fossil fuel power plants generating electricity to drive the system) is dominant for most applications, it is important to be able to accurately determine performance merits of different fluids, and in particular their performance potential in optimized equipment. The goal of this study was to develop optimized refrigerant circuitry designs for R600a (isobutane), R290 (propane), R134a, R22, R410A, and R32 finned-tube evaporators and to analyze the effect of optimized circuitry on evaporator and system performance for these refrigerants.

Studies concerned with optimization of finned-tube heat exchangers have typically been involved in evaluating coils with different pre-selected refrigerant circuits. For example, Casson et al. [1] presented a simulation study, in which they evaluated the performance of R22 alternatives in an optimized condenser and its effect on the system's efficiency. Their results showed that high-pressure refrigerants can be used more effectively with

higher mass fluxes than R22 because of their small drop of saturation temperature for a given pressure drop. Their conclusions supported the results of Cavallini et al. [2] who presented condensation heat transfer data for different fluids at the same so called penalty factor, which takes into account a refrigerant's saturation temperature drop during forced convection condensation. Liang et al. [3] investigated six pre-selected circuitry arrangements using a simulation model. They concluded that a 5% savings in heat transfer surface area is possible with a proper design of the refrigerant circuit.

Granryd and Palm [4] performed an analytical study on the optimum number of parallel sections in an evaporator, and presented their results in terms of a drop in refrigerant saturation temperature. They concluded that for optimum operation the drop of saturation temperature should be 33% of the average temperature difference between the refrigerant and the tube wall, although the result was dependent on the used refrigerant heat transfer and pressure drop correlations.
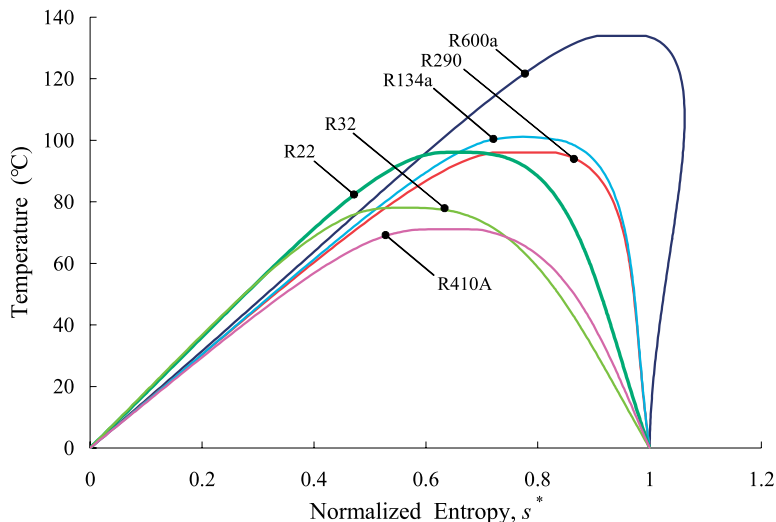

Fig. 1. Temperature–entropy diagram for studied refrigerants (entropy is normalized to the width of the two-phase dome, i.e. $s_f*=0$ and $s_g*=1$).

Table 1
Refrigerant information

Refrigerant	P_g (kPa)	ρ_f (kg m^{-1})	ρ_g (kg m^{-1})	h_{fg} (kJ kg^{-1})	k_f (W m^{-1} K^{-1})	μ_f	dT_{sat}/dP (K kPa^{-1})	Safety designation[a]	GWP[b] (100 years)
R600a	199.5	5.34	572.2	348.2	0.0958	183.05	0.1477	A3	20
R134a	374.6	18.32	1271.3	193.2	0.0889	243.88	0.0770	A1	1320
R290	584.4	12.69	519.0	364.5	0.1024	116.89	0.0585	A3	20
R22	621.5	26.35	1257.3	199.3	0.0916	200.13	0.0516	A1	1780
R410A	995.0	38.19	1141.7	212.6	0.1056	154.92	0.0329	A1/A1	2000
R32	1011.5	27.56	1030.6	304.0	0.1398	139.24	0.0322	A2	543

Thermophysical properties are for saturation temperature of 7.0 °C; based on REFPROP, Ref. [5].
[a] Ref. [6].
[b] Ref. [7,8].

2. Refrigerant studied

Table 1 presents the studied refrigerants in the order of their saturation vapor pressure corresponding to 7.0 °C dew-point temperature. The selected refrigerants have vastly different properties. The liquid conductivity and viscosity of the studied refrigerants, the most influential properties for refrigerant's heat transfer and pressure drop, differ by as much as 15 and 110%, respectively. Greater differences, however, are seen in the thermodynamic properties: the vapor densities differ by up to a factor of 7, dT_{sat}/dP differ by as much as a factor of 4.6, and the latent heats differ by as much as 80%. These properties are related to refrigerant's critical temperature and the shape of the two-phase dome. They affect the selection of the optimal refrigerant mass flux in the refrigerant circuitry and, as we will present it in the later section, refrigerant's COP in the vapor compression cycle. Fig. 1 shows a temperature–entropy diagram using a normalized entropy scale to facilitate qualitative comparison of impact of thermodynamic properties on the COP for the studied refrigerants.

3. Simulation and optimization tools

In this study, we used an evaporator simulation model EVAP from the EVAP-COND simulation package of NIST [9]. Heat exchanger simulations by EVAP are organized in a tube-by-tube scheme allowing the user to specify arbitrary refrigerant circuitry architectures and a one-dimensional distribution of the inlet air. The program recognizes each tube as a separate entity for which it calculates heat transfer. When the refrigerant in a tube changes from two-phase to a superheated vapor, the model locates the transition point between the two phases in the tube and applies appropriate heat transfer and pressure drop correlations to the respective sections of the tube.

For the purpose of this study we examined and updated EVAP's refrigerant heat transfer and pressure drop correlations. From several good choices, we implemented the updated Kattan–Thome–Favrat correlation [10] for the

flow boiling heat transfer coefficient. For pressure drop calculations we chose the correlation by Müller-Steinhagen and Heck [11]. This correlation was rated as one of the top two out of seven correlations by Ould Didi et al. [12] when checked against their 788 data points based on two tube diameters and five refrigerants, irrespective of the flow pattern. We also compared nine correlations against the predictions by the modified Pierre correlation [13], which was successfully applied to evaporation and condensation pressure drop data obtained from three independent laboratories and covering seven refrigerants and two tube diameters. Fig. 2 shows that the Müller-Steinhagen and Heck correlation agrees very well with the modified Pierre correlation. Compared to the Müller-Steinhagen and Heck correlation, the Pierre correlation has the disadvantage that it is not applicable to adiabatic flows. Also, the Pierre correlation calculates the overall pressure drop in a heat exchanger and cannot predict local pressure drop values, especially at high quality range approaching the saturated line.

To obtain capacity predictions for an optimized evaporator for each refrigerant, we ran evaporator simulations using a novel optimization system called intelligent system for heat exchanger design (ISHED1) [14]. It includes the evaporator model EVAP, the control module, and two modules: the knowledge-based evolutionary computation module and the symbolic learning-based evolutionary computation module. These two modules guide the evolutionary process according to the concept referred to as the learnable evolution model, or LEM [15]. The novelty of LEM methodology is that it combines a conventional evolution program with a non-Darwinian evolutionary computation employing symbolic learning.

Consistent with a conventional evolutionary computation approach, ISHED1 operates on one population (generation) of refrigerant circuitry designs at a time. The number of populations to be examined and the number of members per population (refrigerant circuitry designs) are determined by the user at the outset of an optimization run. Each member of the population is evaluated by EVAP, which simulates its performance and provides its cooling
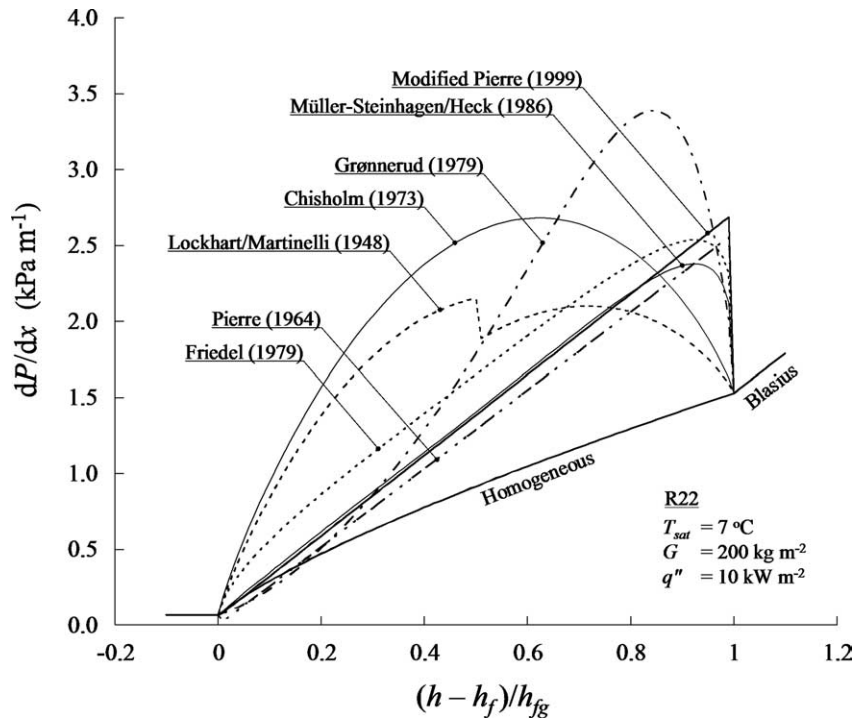
Fig. 2. Comparison of nine pressure drop correlations.

capacity as a single numerical fitness value. The designs and their fitness values are returned to the control module as an input for deriving the next generation of circuitry designs. Hence, the implemented process is a loop, and it is repeated for the number of populations specified by the user at the outset of the optimization run.

4. Evaporator performance with selected refrigerants

Table 2 shows the evaporator design data that was common for all evaporator simulations in this study.

Table 2
Evaporator design information

Items	Unit	Value
Tube length	mm	500
Tube inside diameter	mm	9.2
Tube outside diameter	mm	10.0
Tube spacing	mm	25.4
Tube row spacing	mm	22.2
Number of tubes per row		12
Number of depth rows		3
Fin thickness	mm	0.2
Fin spacing	mm	2
Tube inner surface		Smooth
Fin geometry		Louver
Air volumetric flow rate	$m^3\,min^{-1}$	25.5

Additionally, the air condition was 26.7 °C dry-bulb temperature and 50% relative humidity. The refrigerant inlet condition was specified in terms of the saturation temperature and subcooling at the inlet to the distributor, which was included in the simulation runs. We used subcooling of 5.0 K in all simulations. With specified inlet parameters and environmental conditions, EVAP iterated refrigerant mass flow rate to arrive with a 5.0 K refrigerant exit superheat for the specified exit saturation temperature.

The first simulation task was to obtain evaporator capacity for each refrigerant at the same exit saturation temperature of 7.0 °C. Because of significant differences in thermophysical properties, refrigerant circuitry had to be optimized for each refrigerant. We started by manually developing five basic circuitry architectures involving 1, 1.5, 2, 3, and 4-circuits, four of which are shown in Fig. 3. Then we used ISHED1 for further refrigerant circuitry optimization specifying 15 members per population and 300 populations for each optimization run. Hence, each optimization run included 4500 calls to EVAP. The 1.5, 2, 3, and 4-circuit designs were included as 'seed' designs in the first population. The remaining 11 designs of the first population were developed by ISHED1.

Fig. 4 presents capacity results for the prearranged 1, 1.5, 2, 3, 4-circuit designs and the optimized designs developed by ISHED1. For each refrigerant, the design developed by ISHED1 outperformed the best of the prearranged designs. For R32, R410A, R290, and R22, ISHED1 developed
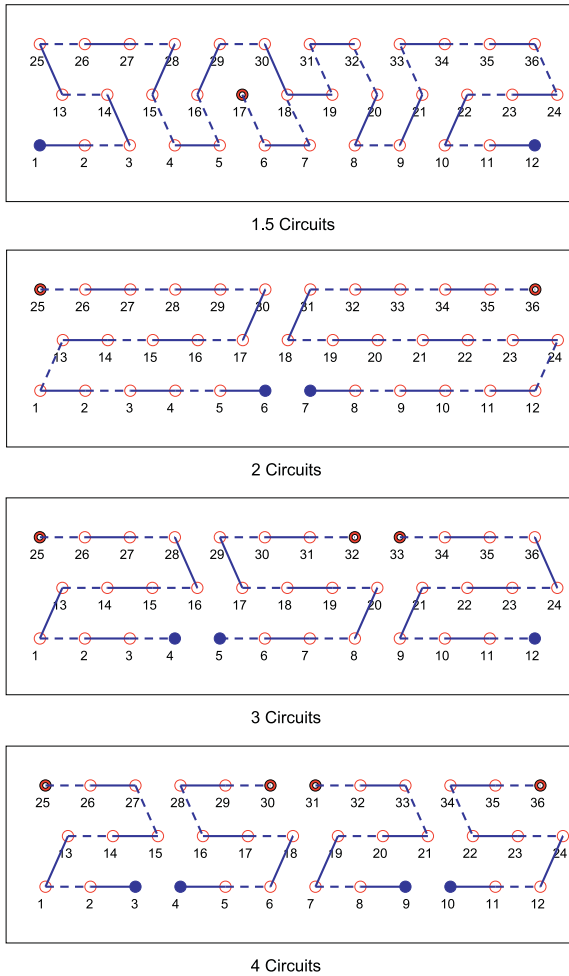
Fig. 3. Manually developed 1.5, 2, 3, and 4-circuit designs (side view; circles denote tubes; continuous lines indicate return bends on the near side of the heat exchanger, broken lines indicate return bends on the far side, full circles indicate outlet tubes).

individually optimized designs, which were based on a 1.5-circuit. Although each of these designs had a somewhat different layout, EVAP simulations confirmed that they were equivalent in performance. For this reason, only the R410A 1.5 circuitry ISHED1-developed design was used further for R32, R410A, R290, and R22. For R134a and R600a, a 3-circuit and a 4-circuit design, respectively, were proposed by ISHED1. Fig. 5 presents the 1.5, 3, and 4-circuit designs developed by ISHED1.

EVAP simulations using ISHED1 optimized evaporators generated the results presented in Table 3. For comparative evaluation, we selected R22 as our reference. R600a had the lowest capacity, 9.5% below that of R22, and R32 had the highest capacity exceeding that of R22 by 14.5%. We also should note that the low-pressure refrigerants, R600a and R134a, had the lowest ratio of the latent capacity to total capacity.
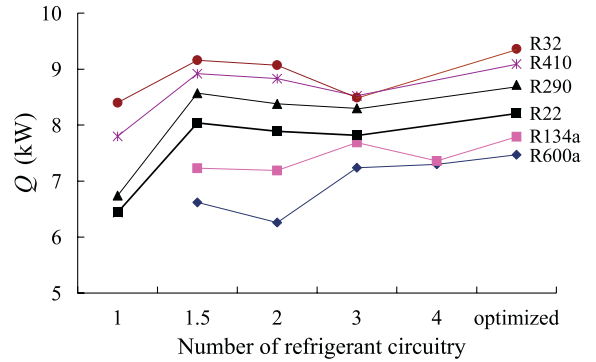

Fig. 4. Evaporator capacities for manually developed and ISHED1-optimized circuitry designs.

5. Impact of evaporator performance on system COP

We used the basic thermodynamic analysis of the vapor compression cycle, as implemented by the CYCLE_D model [16], to assess the impact that the evaporator performance has on the COP for different refrigerants. In the CYCLE_D simulations, refrigerant saturation temperatures in the evaporator and condenser are specified as input. To acquire all of the data, we performed two rounds of simulations. In the first round, we used the same evaporator exit saturation temperature, T_{sat}, of 7.0 °C for each
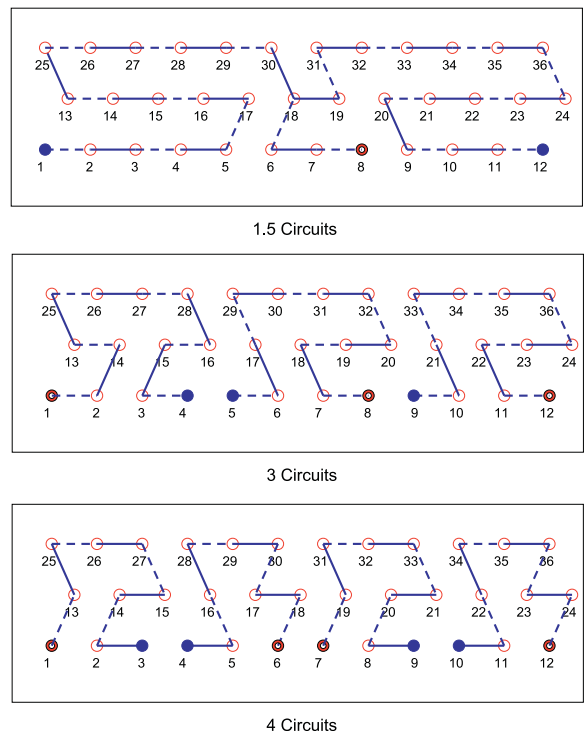

Fig. 5. 1.5-Circuit, 3-circuit and 4-circuit designs optimized by ISHED1.

Table 3
Summary of simulation results for ISHED1-optimized designs for $T_{sat} = 7.0\,°C$

Refrigerant	Number of circuits	x_{in} (–)	P_{out} (kPa)	ΔP (kPa)	ΔT_{sat} (K)	m_r (kg h^{-1})	Q (kW)	Q_l/Q	Q/Q_{R22}
R600a	4	0.26	200	12	1.7	102.0	7.430	0.18	0.905
R134a	3	0.27	375	27	2.0	195.6	7.787	0.20	0.948
R290	1.5	0.27	585	59	2.8	116.1	8.706	0.23	1.060
R22	1.5	0.23	621	64	3.2	190.7	8.211	0.21	1.000
R410A	1.5	0.29	993	57	1.8	213.5	9.091	0.25	1.107
R32	1.5	0.24	1012	40	1.3	143.0	9.399	0.26	1.145

Table 4
Input data to CYCLE_D

Inputs	Unit	Data
Compressor isentropic efficiency		0.65
Compressor volumetric efficiency		0.82
Electric motor efficiency		0.85
Suction line pressure drop[a]	°C	1.0
Discharge line pressure drop[a]	°C	1.0
Evaporator superheat	°C	5.0
Condenser subcooling	°C	5.0
LL-SL heat exchanger		None

[a] Pressure drop corresponding to saturation temperature change.

refrigerant. For the second round, we first performed iterative EVAP simulations at various evaporator saturation temperatures to obtain a capacity equal to that of R22 at 7.0 °C saturation temperature. The obtained saturation temperatures, constituted a new input for each refrigerant (instead of 7.0 °C) for the second round of CYCLE_D simulations.

We performed simulations at two condensing temperatures of 38.0 and 45.0 °C. Table 4 contains the additional CYCLE_D input used in these calculations, and Table 5 presents the obtained results for the two rounds of

simulations. The results in the left-hand-side of the table, with $T_{sat} = 7.0\,°C$, are from the basic thermodynamic calculations of the cycle. The results located in the right-hand-side of the table, with different values of T_{sat}, account for the impact that the thermodynamic and transport properties have on the cycle through their effect on the performance of the optimized evaporator.

Fig. 6 presents COP results referenced to the COP of the baseline R22 cycle. As expected, COPs for theoretical simulations in the basic cycle ranked the refrigerants in the order of their critical temperatures (Fig. 1). For the condensing temperature of 38 °C, COP of R600a is 5.3% better than that of R22, and the COP of R32 is 5.1% worse. However, the performance of the group was found to be much more uniform when the effects of the optimized evaporators and corresponding saturation temperatures are included in the simulations. While propane arrived as the most efficient refrigerant with a 3.5% better COP than R22, the COPs of the remaining refrigerants were found to be within 0.7% of the COP of R22. The high-pressure (low critical temperature) R32 experienced the greatest COP improvement when evaporator effects were taken into account, and in relation to R600a it changed the 10.4% COP deficit to 0.8% advantage. All refrigerants provided

Table 5
Performance for the theoretical cycle and the cycle accounting for evaporator effects

Refrigerant	Basic theoretical cycle[a]		Cycle including evaporator effects		
	T_{sat} (°C)	COP	T_{sat} (°C)	COP	Q_l/Q
38.0 °C Condensing temperature					
R600a	7.0	4.103	5.7	3.895	0.22
R134a	7.0	3.993	6.4	3.896	0.22
R290	7.0	3.929	7.7	4.036	0.21
R22	7.0	3.898	7.0	3.898	0.21
R410A	7.0	3.703	8.1	3.874	0.21
R32	7.0	3.701	8.5	3.926	0.21
45.0 °C Condensing temperature					
R600a	7.0	3.237	5.8	3.111	0.22
R134a	7.0	3.133	6.4	3.064	0.22
R290	7.0	3.074	7.8	3.155	0.21
R22	7.0	3.063	7.0	3.063	0.21
R410A	7.0	2.869	8.2	2.995	0.21
R32	7.0	2.878	8.5	3.073	0.21

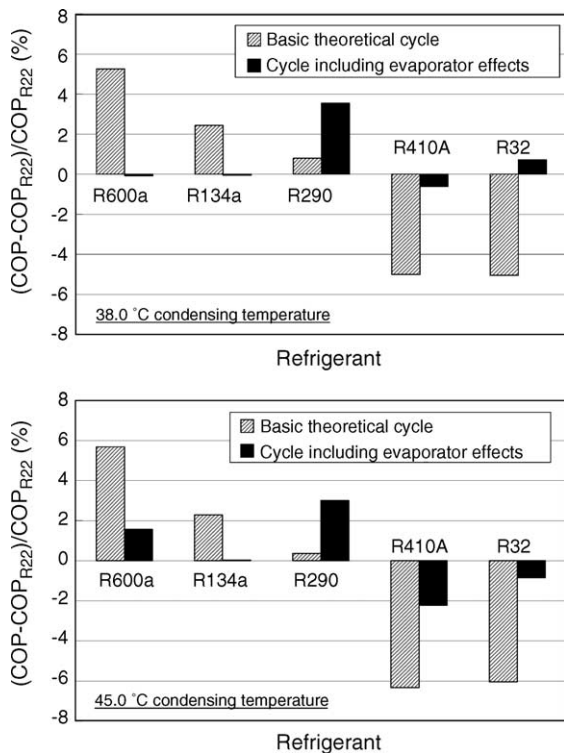[a] Using the same evaporating temperature.

Fig. 6. COPs compared to the COP of R22 for the basic cycle and for the cycle including evaporator effects for 38.0 and 45.0 °C condensing temperatures.

similar latent capacities. The results for the 45.0 °C condensing temperature display similar trends with the difference that the high-pressure refrigerants (R32 and R410A) showed somewhat lower performance because the cycle moved closer to their critical points.

6. Concluding remarks

Comparable theoretical evaluations of refrigerants in a vapor-compression cycle using thermodynamic properties alone tend to yield a better COP for low-pressure refrigerants (having a high critical temperature) versus high-pressure refrigerants (having a low critical temperature). This is due to smaller irreversibilities realized in a cycle at given evaporating and condensing temperatures when it operates far away from the refrigerant's critical point. The COP advantage shown by such theoretical evaluations for low-pressure refrigerants does not, however, account for the advantage high-pressure fluids have in optimized finned-tube heat exchangers. For the same cooling capacity, high-pressure refrigerants tend to have a higher saturation temperature at the evaporator exit than low-pressure refrigerants, which can compensate for the theoretical cycle inferiority high-pressure fluids may have.

In this study, we evaluated the performance of R600a, R134a, R290, R22, R410A, and R32, which differ vastly in critical temperatures and other thermophysical properties. We optimized evaporator circuitry for each refrigerant using a non-Darwinian evolutionary scheme, and performed simulations of the optimized evaporators. The high-pressure refrigerants provided higher evaporator capacities than the low-pressure refrigerants. For a 7.0 °C evaporator exit saturation temperature, and using R22 as a reference, R32, R410A, and R290, had a greater capacity by 14.5, 10.7, and 6.0%, while R134a and R690a had a lower capacity by 5.2 and 9.5%, respectively. The subsequent theoretical cycle simulations with the same 7.0 °C evaporator saturation temperature showed the COPs of the studied refrigerants to be in the order of their critical temperatures, i.e. low-pressure refrigerants had the best COPs. However, for the cycle simulations including evaporator effects (carried out at a different evaporator saturation temperature for each fluid to match the R22 capacity), the refrigerants performed within approximately a 2% band of the R22 COP baseline for the two condensing temperatures used. The exception to this was R290, whose COP was better than that of R22 by approximately 3% due to a set of favorable thermophysical properties. It is worth noticing that R32 overcame the 10% COP deficit it had in the theoretical cycle in reference to R600a and showed a comparable performance when evaporator effects were included in the cycle simulation.

It must be emphasized that this study isolated the evaporator effects, and did not include similar effects that may be introduced by the condenser. Also, we have to note that selection of the compressor and relative sizing of the remaining components will affect the performance of a complete system. This study was not concerned with design tradeoffs and the cost related to the practical implementation of different refrigerants, e.g. safety considerations for flammable refrigerants, equipment size, pressure, or lubricant issues. The condensing and evaporating temperatures used in this study correspond to the comfort cooling application. An additional insight could be obtained from a similar study performed at the same reduced temperatures for the considered refrigerants.

References

[1] V. Casson, A. Cavallini, L. Cecchinato, D. Del Col, L. Doretti, E. Fornasieri, et al., Performance of finned coil condensers optimized for new HFC refrigerants, ASHRAE Trans 108 (2) (2002) 517–527.

[2] A. Cavallini, D. Del Col, L. Doretti, L. Rossetto, Condensation heat transfer of new refrigerants: advantages of high pressure fluids, Eighth international refrigeration conference at Purdue University, West Laffayette, IN, 2000.

[3] S.Y. Liang, T.N. Wong, G.K. Nathan, Numerical and experimental studies of refrigerant circuitry of evaporator coils, Int J Refrigeration 24 (8) (2001) 823–833.

[4] E. Granryd, B. Palm, Optimum number of parallel sections in evaporators, 21st International congress of refrigeration, paper ICR0077, IIR/IIF, Washington, DC, 2003.

[5] E.W. Lemmon, M.O. McLinden, M.L. Huber, NIST reference fluids thermo-dynamic and transport properties—REFPROP 7.0. Standard reference database 23, National Institute of Standards and Technology, Gaithersburg, MD; 2002.

[6] ASHRAE, ANSI/ASHRAE Standard 34-2001, Designation and safety classification of refrigerants. American society of heating, refrigerating, and air-conditioning engineers, Atlanta, GA, 2001.

[7] J.M. Calm, G.C. Hourahan, Refrigerant data summary, Eng Syst 18 (11) (2001) 74–88.

[8] IPCC, Climate change 2001: the scientific basis—contribution of working group I to the IPCC third assessment report, Intergovernmental panel on climate change of the world meteorological organization and the United Nations Environment Programme (UNEP), Cambridge University Press, Cambridge, UK, 2001.

[9] NIST, Simulation models for finned-tube heat exchangers— EVAP-COND, National Institute of Standards and Technology, Gaithersburg, MD, 2003. http://www2.bfrl.nist.gov/software/evap-cond/.

[10] J.R. Thome, Update on advances in flow pattern based two-phase heat transfer models, Experimental Thermal and Fluid Science 29 (3) (2005) 341–349.

[11] H. Müller-Steinhagen, K. Heck, A simple friction pressure drop correlation for two-phase flow in pipes, Chem Eng Process 20 (6) (1986) 297–308.

[12] M.B. Ould Didi, N. Kattan, J.R. Thome, Prediction of two-phase pressure gradients of refrigerants in horizontal tubes, Int J Refrigeration 25 (7) (2002) 935–947.

[13] J.Y. Choi, M.A. Kedzierski, P.A. Domanski, Generalized pressure drop correlation for evaporation and condensation in smooth and micro-fin tubes, IIR commission B1 conference, thermophysical properties and transfer processes of new refrigerants, Paderborn, Germany; October 3–5, 2001.

[14] P.A. Domanski, D. Yashar, K.A. Kaufman, R.S. Michalski, Optimized design of finned-tube evaporators using learnable evolution methods, Int J HVAC&R Res 10 (2) (2004) 201–212.

[15] R.S. Michalski, Learnable evolution model: evolutionary process guided by machine learning, Machine Learning 38 (1) (2000) 9–40.

[16] P.A. Domanski, D.A. Didion, J. Chi, NIST vapor compression cycle design program—CYCLE_D 3.0, Standard reference database 49, National Institute of Standards and Technology, Gaithersburg, MD, 2003.